

# Mithril: Cooperative Row Hammer Protection on Commodity DRAM Leveraging Managed Refresh

Michael Jaemin Kim, Jaehyun Park, Yeonhong Park, Wanju Doh,  
Namhoon Kim, Tae Jun Ham, Jae W. Lee, and Jung Ho Ahn

Seoul National University

geniajh@gmail.com

**Abstract**—Since its public introduction in the mid-2010s, the Row Hammer (RH) phenomenon has drawn significant attention from the research community due to its security implications. Although many RH-protection schemes have been proposed by processor vendors, DRAM manufacturers, and academia, they still have shortcomings. Solutions implemented in the memory controller (MC) pay an increasingly higher cost due to their conservative design for the worst case in terms of the number of DRAM banks and RH threshold to support. Meanwhile, the DRAM-side implementation has a limited time margin for RH protection measures or requires extensive modifications to the standard DRAM interface.

Recently, a new command for RH protection has been introduced in the DDR5/LPDDR5 standards, called *refresh management (RFM)*. RFM enables the separation of the tasks for RH protection to both MC and DRAM. It does so by having the former generate an RFM command at a specific activation frequency, and the latter take proper RH protection measures within a given time window. Although promising, no existing study presents and analyzes RFM-based solutions for RH protection. In this paper, we propose Mithril, the *first* RFM interface-compatible, DRAM-MC cooperative RH protection scheme providing deterministic protection guarantees. Mithril has minimal energy overheads for common use cases without adversarial memory access patterns. We also introduce Mithril+, an extension to provide minimal performance overheads at the expense of a tiny modification to the MC while utilizing an existing DRAM command.

## I. INTRODUCTION

DRAM has been an essential part of computer systems for decades. One characteristic of DRAM is that DRAM inherently leaks charges over time. Thus an auto-refresh command needs to recharge a DRAM cell at an interval of refresh window to avoid a loss of data. However, when a certain row (aggressor) is activated at a rate surpassing a certain threshold, the nearby row (victim) may experience a bit flip phenomenon. This reliability problem is called *Row Hammer (RH)* [28], [29] and the threshold number of activations within a single refresh window causing the first-bit flip is called *RH-threshold* ( $RH_{TH}$ ). Unfortunately, the RH problem is becoming more critical as fabrication technology scales [14]. Recent works report  $RH_{TH}$  to be as low as 20K, and several literatures identified that even non-adjacent victim rows could be influenced by the RH phenomenon [15], [28].

The RH phenomenon has been a serious security vulnerability as it breaks the basic integrity guarantee in the

computer system. RH-induced bit-flip can be abused in various attack scenarios. For example, the RH can be utilized to modify an unauthorized memory location or enable other attack techniques such as privilege escalation and cross-VM attacks [1], [11], [12], [17], [41], [49], [53].

The criticality of this problem motivated many RH protection solutions. There exist several software-based solutions [5], [9], [19], [30], [49], but such solutions often incur a high-performance cost and have limited coverage (i.e., only effective against a specific attack scenario). For these reasons, architectural solutions have emerged as promising alternatives.

By providing the RH mitigation at the DRAM device level, these mechanisms can provide strong protection against most attack scenarios with relatively low or negligible performance overhead. Most architectural RH defense solutions exploit one of the two mechanisms: adjacent row refresh (ARR) and memory access throttling. *ARR* [29], [31], [39] is a non-standard DRAM command that is issued by memory controllers to initiate an extra preventive refresh ( $REF_{prev}$ ) on potential RH victim rows. *Throttling* [16], [50] is a mechanism of limiting the overly frequent activations on the potential RH aggressor row from the memory controller.

Using one of the remedies, existing architectural RH-protection schemes provide either *probabilistic* or *deterministic* protection guarantee for the target  $RH_{TH}$ . The probabilistic protection schemes are efficient in that they often require very few extra structures, but they cannot completely prevent the RH attack. On the other hand, the deterministic protection schemes utilize an extra counter structure to track the potential RH aggressor rows to provide the complete protection guarantee. Often, *streaming algorithms* (Section II-F) or *grouped-counter approaches* are utilized to effectively manage the counter table.

One of the important design decisions for the architectural RH-protection scheme is where to implement the proposed solution within the system. In practice, most RH protection solutions are either implemented in an on-die memory controller (MC) or a DRAM device. For example, Graphene [39], BlockHammer [50], and PARA [29] are implemented in the on-die MC, whereas TWiCe [31] and the industry-oriented RH protection schemes [14], [37] are implemented in the DRAM. Unfortunately, both choices have their own drawbacks.

First, the MC-side implementation needs to provide RH protection resources for the worst-case, where the expected  $RH_{TH}$  level is very low, and the processor is connected to the maximum number of DRAM banks it supports. As a result, it requires a large extra area for the counter structures that the RH protection mechanism utilizes.

The DRAM-side implementations are free from such concerns, as  $RH_{TH}$  of a specific DRAM is estimated accurately by DRAM vendors, and the resource usage is proportional to the number of DRAM banks since on-DRAM RH-protection schemes are often deployed at a per-bank or per-DIMM basis. However, such on-DRAM protection schemes suffer from the *deployability* issues.

To secure the time margin for the extra  $REF_{prev}$  for the potential RH victim rows, the DRAM-side schemes must either request the MC to generate the non-standard ARR commands or perform extra  $REF_{prev}$  during the auto-refresh in a way that is transparent to the MC. The former mechanism breaks the abstraction that DRAM is a passive device. In contrast, the latter mechanism [14] called the time-margin-stealing method is not always possible depending on the DRAM characteristics and the auto-refresh margin.

*Refresh Management (RFM)* is a new candidate for a remedy in addition to the prior ARR and throttling, which has been newly introduced to the DDR5 and LPDDR5 specifications [21], [22]. An MC sends an RFM command at a specific activation frequency to a target DRAM bank without a target row. The DRAM-side RH-protection scheme can exploit the time margin provided by the RFM command to take necessary actions, typically extra  $REF_{prev}$ . This cooperation between the MC and DRAM effectively avoids the critical drawbacks of MC- or DRAM-only implementations.

Despite its promising trait, the applicability of RFM for the RH-protection scheme has not been publicly verified or appropriately evaluated to the best of our knowledge. A prior probabilistic scheme [29] may be trivially applied. However, the prior deterministic schemes cannot be directly applied to the RFM interface. The prior ARR-based schemes *reactively* issue the command targeting a specific row when the activation count reaches a scheme-specific *predefined threshold*. However, periodic in its nature, the RFM command is prone to the worst case where multiple rows simultaneously require the  $REF_{prev}$  in a short time period, unlike the ARR command. Throttling-based prior work also cannot utilize the RFM command properly. Thus, prior ARR- or throttling-based RH-protection schemes are inefficient over the RFM-interface.

Mithril, a novel DRAM-side, RFM-compatible, and deterministic RH-protection scheme takes a new approach in utilizing the RFM command. To avoid such a concentration of rows to refresh, we take a *greedy approach* in selecting the target row to refresh at every RFM command. Moreover, we investigate the usage of the streaming algorithms and grouped counter approaches from the prior works to finally construct an effective method to manage the counter structure. We provide a new mathematical proof that by simply maintaining the greedy selection for  $REF_{prev}$ , we guarantee deterministic

TABLE I  
SYMBOLS AND THEIR DESCRIPTIONS USED FOR DRAM REFRESH, ROW HAMMER, AND STREAMING ALGORITHM.

Symbol	Description
tREFW	Per row auto-refresh interval (e.g. 32ms and 64ms)
$RH_{TH}$	Notation for RH threshold.
$REF_{prev}$	Extra preventive refresh on the potential RH victim rows. Executed during ARR, RFM command, or hidden in the auto-refresh.
$r_{blast}$	Distance that RH effect reaches.
$Real_{cnt}$	Real number of occurrence in a data stream.
$Est_{cnt}$	Reported number of $Real_{cnt}$ from the algorithm.

protection against a target  $RH_{TH}$ . Finally, we propose 1) algorithmic optimization for energy saving, 2) RFM extension to mitigate performance overhead by exploiting the memory access patterns of the ordinary workloads, and 3) hardware optimization that obviates the need for counter table reset, which was mandatory in the prior work.

The key contributions of this paper are as follows:

- We classify the possible combinations of different streaming algorithms and remedies for RH-protection and investigate appropriate methods for the RFM-based scheme.
- We propose Mithril, the first RFM-based RH-protection scheme with deterministic safety guarantees, exploiting a modified Counter-based Summary algorithm.
- We provide a rigorous mathematical proof of the modified algorithm and the RH safety of Mithril.
- We suggest the energy and performance optimization techniques that exploit the memory access patterns of the common, non-adversarial workloads.

## II. BACKGROUND

### A. DRAM Refresh

DRAM stores a single bit in a *cell*, composed of one capacitor and one access transistor. These cells are organized into *rows* and *columns*. A DRAM row, which shares a wordline, is the granularity of the *activation* (ACT) and *precharge* (PRE), which respectively allows and disallows the *read* or *write* operation on the row. The read and write operation occurs by accessing a certain number of columns in an activated row. DRAM is composed of multiple *banks*. Each bank allows independent ACT, PRE, read, and write operations. Multiple banks form a *rank*, which shares the memory channel to the memory controller (MC) at the host side.

Due to the inherent characteristic of a DRAM cell capacitor that the stored charge leaks over time, the cell value needs to be restored periodically [6], [8]. This periodic restoration is called *auto-refresh* and is initiated at every refresh (REF) command within tRFC (refresh time) period. Every DRAM row must be refreshed at least once every refresh window (tREFW) to be safe from such a charge retention problem. In modern DRAM devices (e.g., DDR5 [22]), all the rows in a single bank are divided into typically 8,192 groups. A group is refreshed every time interval tREFI (refresh interval).

### B. Row Hammer Phenomenon

Row Hammer (RH) refers to a phenomenon that repetitive activations of a specific row (aggressor) lead to bit flips in its physically nearby rows (victim) [29], [36], [38], [51]. A bit flip is observable when the activation count reaches a certain RH threshold ( $RH_{TH}$ ) without being refreshed inside a tREFW time window. The  $RH_{TH}$  value varies depending on different chips, generations, or DRAM manufacturers [28]. The RH problem is getting worse following the current trend of fabrication technology scale-down, ensued by the intensified inter-cell interference. Recent studies [14], [28] reported that  $RH_{TH}$  has reduced to mere several thousand ACTs. It has also been observed that non-adjacent rows affect the victim rows when activated frequently. We refer to the distance between the aggressor and victim as blast radius ( $r_{blast}$ ) [50].

### C. Remedies and Protection Guarantees for RH

There have existed two types of remedies prior to the refresh management (RFM) command: ARR and throttling. **ARR** refers to a type of commands that the MC issues to DRAM with an explicit *target row address* (either aggressor or victim) at a *required moment*. It triggers an extra  $REF_{prev}$  on the potential RH victim rows within the time margin the command provides. It is different from the normal REF command, which is row agnostic and periodic. A command with a similar concept was once proposed in DDR4 [20] but is now deprecated. Prior RH-protection schemes that exploited ARR either issued the command based on some *probability* [29], [46], [52] or when the ACT count of a certain aggressor exceeds a scheme-specific *predefined threshold*, being assumed hazardous.

**Throttling** is a method where MC *delays* the frequency of activation on an aggressor starting at the moment of identification for a defined time. The duration and intensity of the delay are adjusted to guarantee RH protection. [16] first suggested such a methodology, and [50] proposed a deterministic RH-protection scheme utilizing the throttling method.

There exist two different types of RH-protection guarantees: deterministic and probabilistic. **Deterministic** guarantee ensures the RH-protection by guaranteeing that a victim row is always refreshed before it is affected by the ACT more than  $RH_{TH}$ , either by the extra  $REF_{prev}$  or the normal auto-refresh. It utilizes a counter structure to track the aggressor row and executes one of the two remedies promptly. The main drawback of the deterministic scheme is its higher area overhead. Given that the counter structure dominates the overall area cost, representative prior works have either utilized a streaming algorithm [31], [39], [50] or a grouped counter approach [25], [43] to minimize its size.

**Probabilistic** guarantees prevent RH with a certain probability. The probabilistic approach has its strengths in the minimal area overhead. However, the performance overhead exacerbates severely when the target  $RH_{TH}$  level is lowered or when the number of DRAM devices in the system increases. It does not provide a deterministic protection guarantee either.

### D. Implementation Location

Architectural RH-protection schemes can be located either on the MC-side or the DRAM-side. **MC-side implementation** has its strength in that it utilizes a superior logic process with a higher area budget available. However, it has major drawbacks. It demands 1) a conservatively high number of counter structures to allocate, 2) a conservatively low target  $RH_{TH}$  value, and 3) MC modification with higher complexity.

The counter table of the deterministic scheme is typically allocated per DRAM bank. The latest CPU servers, such as Intel Ice Lake, support up to 2048 banks per socket (8 channels  $\times$  8 ranks  $\times$  32 banks). This number could further increase if we consider 3D stacked DRAM devices or future generations. Even though fully populating 2048 banks may be unlikely, the counter structures must be designed to support the worst case. Such limitation was not properly taken into account by the prior works such as BlockHammer [50] and Graphene [39], which only report the area overhead of the counter table for 16 DRAM banks.

The target  $RH_{TH}$  value to protect against varies greatly depending on the manufacturer, generation, or even device. Considering that most deterministic schemes have to be tuned to the target  $RH_{TH}$  at design time, it must be built to protect against the pessimistic  $RH_{TH}$  value. The MC-side schemes also often demand new commands that have to be issued in an interrupt-like manner [39], [43] or require a new MC scheduler and system support [50].

Throttling is only practical on the MC side, physical isolation [9], [30], [49] is too costly, and the higher refresh rate [4], [29] is limited in its protection guarantee. Therefore, **DRAM-side implementation** typically relies on the extra  $REF_{prev}$  on the potential RH victim row. To secure the uninterrupted time to execute the  $REF_{prev}$ , prior DRAM-side RH-protection schemes had to rely on either the *feedback-augmented* ARR command or the auto-refresh time-margin stealing method.

The former is similar to the normal ARR command issued by MCs but requires that DRAM halt the MC for a certain amount of time. There exists some method of feedback from DRAM to MC, such as ALERT\_n signal, but requires more pin to deliver additional alert types to support the DRAM-side RH-protection scheme. The latter method, auto-refresh time margin stealing, invisibly executes  $REF_{prev}$  during normal auto-refresh. Albeit not requiring any feedback path, it has a limited amount of time margin that can be stolen, thus cannot be scaled to a low  $RH_{TH}$  value.

### E. RFM Interface as a New Remedy

Under these circumstances, the RFM interface has been newly introduced as an *alternative remedy* that allows for *DRAM-MC cooperation*. It is suggested as the primary means of RH-protection by the JEDEC committee [23], [24]. The RH-protection scheme resides on the DRAM-side while the MC provides a periodic but DRAM-row agnostic time margin to the DRAM bank. Periodic here means that it is not based on time but the number of ACTs on a single DRAM bank. Figure 1 shows an exemplar main-memory organization using

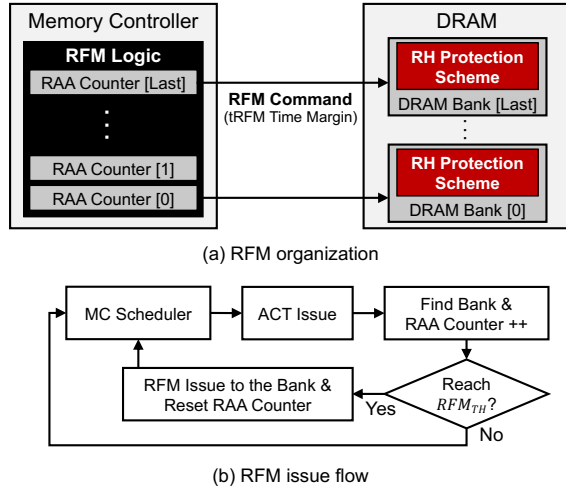


Fig. 1. (a) Exemplar main-memory organization with RFM interface. (b) The issue logic of RFM.

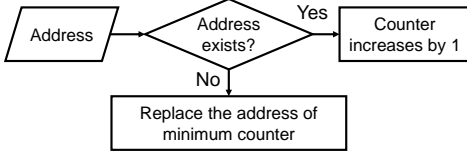


Fig. 2. Counter-based Summary(CbS) algorithm operation.

the RFM interface and RFM issue logic. An MC has a Rolling Accumulated ACT (RAA) counter per bank that keeps track of the number of ACTs on its bank. When the RAA count reaches an RFM threshold ( $RFM_{TH}$ ), the MC issues an RFM command only to the corresponding bank and resets the RAA counter for the target bank. At every RFM command issue, the recipient bank receives a time margin (tRFM) during which no disturbance from any other regular operation is guaranteed. A key difference with the prior ARR command is that RFM is row agnostic and periodic (i.e., it cannot be issued in a bursty way). In a sense, it can be seen as an extension of the time-margin stealing method.

The RFM-based RH-protection scheme can avoid overkill because it can use a more accurate prediction of  $RH_{TH}$  and set the  $RFM_{TH}$  value after testing the manufactured chip. Moreover, the DRAM-side RH-protection scheme can get an additional time margin from the MC without an additional interface for the feedback path. The format of an RFM command is similar to that of a per-bank REF command [21], [22], requiring minimal additional complexity.

#### F. Streaming Algorithms and CbS Algorithm

A sequence of ACTs can be seen as a data stream where each input can be examined only once. Processing dense, fast data streams with limited memory to gain useful information has been researched under the name of the *streaming algorithm* [35] in the field of data mining. Among different subgroups of streaming algorithms, each aiming at extracting a different kind of information from a data stream, the ones estimating the total number of occurrences per input element

fit for RH protection. They report the approximate number of each element's occurrences called estimated count ( $Est_{cnt}$ ) instead of real count ( $Real_{cnt}$ ).

*Counter-based Summary* (CbS) [2], [33], [34] is one of the representative streaming algorithms. The algorithm has a table of entries, each holding an address and a counter. When the queried address hits an entry in the table, the corresponding counter is incremented by one. When it misses the table, it replaces the address of the entry with the minimum counter value in the table with the queried address. Then it increments its counter by one (Figure 2). Due to its monotonically increasing nature and swapping, the accumulated counter value above the minimum in the table belongs to the currently written address. In contrast, the ones below the minimum cannot find their source.

$$\text{On-Table Address: } Real_{cnt} \leq Est_{cnt} = Counter \leq Real_{cnt} + Min \quad (1)$$

$$\text{Off-Table Address: } Real_{cnt} \leq Est_{cnt} = Min \leq Real_{cnt} + Min \quad (2)$$

The CbS algorithm reports the  $Est_{cnt}$  of an on-table address with its written counter value, whereas the  $Est_{cnt}$  of an off-table address with the minimum value in the whole table. Inequalities (1) and (2) show the bound of  $Est_{cnt}$ , with  $Min$  denoting the minimum counter value in the table.

### III. INVESTIGATING RFM-BASED SCHEMES

The probabilistic scheme (e.g., [29]) can be trivially extended to the RFM interface. However, when it comes to the deterministic scheme, we no longer can use the prior ARR-based schemes nor the existing streaming algorithm as-is for the counter table management. We investigate the proper approach for the deterministic RFM-based scheme and the proper method of counter-table management.

#### A. Streaming Algorithm Bounds

The  $Est_{cnt}$  boundary of the streaming algorithm is expressed in two inequalities with regard to the  $Real_{cnt}$  (see the exemplar inequality (1) and (2) of the CbS algorithm). We refer to the left-hand side of the inequality as the bound-low and the right-hand side as the bound-high (Table II). The bound-low shows not only the lower bound of  $Est_{cnt}$  but also the upper bound of  $Real_{cnt}$ , and vice versa. Among the inequality boundaries, there are two types: *deterministic* (*Det*) and *probabilistic* (*Prob*) ones. The *Det* boundary is always met regardless of the input distribution or stream pattern. However, the *Prob* boundary is only satisfied with a certain probability, which is likely to be met at a common case such as uniform or zipfian distribution, while being prone to skewed adversarial patterns.<sup>1</sup> The algorithms can be classified into four

<sup>1</sup>The Count-min Sketch algorithm [10] is representative algorithm with *Prob* bound-high. It keeps a table of counters and uses multiple hash functions. When input data is processed, data is designated to multiple counters pointed by the hash functions, and corresponding counters are incremented. When queried by data, the algorithm reports its  $Est_{cnt}$  as the minimum value among the hash indexed counters, thus is always over-estimated (*Det* bound-low). However, because it utilizes the hash functions, a maliciously skewed data set can cause redundant indexing, resulting in a high minimum and over-estimation (*Prob* bound-high) for a single data address.

TABLE II  
COMBINATIONS OF THREE RH-PROTECTION REMEDIES AND FOUR CATEGORIES OF STREAMING ALGORITHMS.

	bound-low / bound-high				
	Det / Det		Det / Prob	Prob / Det	Prob / Prob
	Lossy-Counting $Real_{cnt} - \epsilon m \leq Est_{cnt} \leq Real_{cnt}$	CbS $Real_{cnt} \leq Est_{cnt} \leq Real_{cnt} + \epsilon m$	Count-min Sketch $Real_{cnt} \leq Est_{cnt} \leq Real_{cnt} + \epsilon   f-a  $	Sticky-Sampling $Real_{cnt} - \epsilon m \leq Est_{cnt} \leq Real_{cnt}$	Count Sketch $Real_{cnt} - \epsilon   f-a   \leq Est_{cnt} \leq Real_{cnt} + \epsilon   f-a  $
ARR	O (TWiCe)	O (Graphene)	X	X	X
Throttle	O	O	O (BlockHammer)	X	X
RFM	?	?	X	X	X

\*  $\epsilon$  indicates an algorithm specific error terminology and  $m$  denotes the length of the total stream (e.g., number of ACTs).  $||f-a||$  denotes the size of the input space (e.g., DRAM row address space), excluding the address of the current  $Est_{cnt}$ .

categories depending on the type of boundaries they possess (see Table II).

### B. Viable Combinations of Remedies and Algorithms

When it comes to applying the streaming algorithm to an RH-protection scheme, first the *bound-low* has to be *Det* to build a deterministic solution. Suppose  $Est_{cnt}$ , the value that the scheme bases its action upon, be lower than  $Real_{cnt}$  unboundedly (i.e., *Prob*). In that case, we cannot guarantee deterministic safety. Thus, algorithms with the *Prob* bound-low cannot be the candidates for deterministic schemes. Moreover, depending on the type of remedy, the requirements for the algorithm are different.

**ARR:** Once ARR is applied to the target victim, the activation  $Real_{cnt}$  of the aggressor becomes zero. Thus, it is necessary to readjust the counter structure (i.e.,  $Est_{cnt}$ ) to minimize the error between  $Est_{cnt}$  and  $Real_{cnt}$ . TWiCe [31], which exploited the Lossy-counting algorithm [32] in retrospect, utilizes the *Det* bound-high of the algorithm.  $Est_{cnt}$  is guaranteed to be lower than  $Real_{cnt}$ ; thus, it can be safely reset to zero following  $Real_{cnt}$  (Table II). Graphene [39], which uses the modified Misra-Gries algorithm [34], exploits a property derived from the *Det* bound-low. When a certain  $Est_{cnt}$  reaches the  $\epsilon m$  value, Misra-Gries guarantees that its address does not get swapped out [39]. Using this property, Graphene does not readjust  $Est_{cnt}$  after ARR. However, it issues ARR at every multiple of the predefined threshold that  $Est_{cnt}$  reaches.

**Throttling:** Unlike ARR, throttling does not require readjustment of  $Est_{cnt}$  since the normal ACT command only alters  $Real_{cnt}$ . Therefore, only the *Det* bound-low is required for the algorithm. Thus, not only the “*Det/Det*” algorithms of Table II are possible to use, but the algorithm of “*Det/Prob*” is available. In fact, BlockHammer [50] used the Count-min Sketch [10] algorithm (or its equivalent counting bloom filter) as a means of counter management.

Count-min Sketch does not require a specific counter table size for a target  $RH_{TH}$  unlike the Lossy-counting or CbS algorithm; it rather can be chosen empirically. However, reducing the table size too much could result in a high rate of false-positive. Moreover, the algorithm is prone to adversarial patterns, given that it is based on the hash function. This can be more detrimental to the throttling-based RH-protection scheme because falsely throttling a benign thread or DRAM row can lead to performance degradation.

It may be tempting to utilize the algorithms with the *Prob* bound-low such as Sticky Sampling [32] or Count Sketch [10], not to the deterministic but the probabilistic RH-protection scheme. They may incur minimal performance overhead compared to the pure sampling with merely a limited area overhead. However, they are prone to adversarial patterns, resulting in a worse probability in the corner cases, just as ProHIT and MRLoc did [39].

### C. RFM and Greedy Selection

An RFM-based scheme requires a new approach in selecting a row to execute  $REF_{prev}$  and manage the counter table. Executing a  $REF_{prev}$  during the RFM is a prominent option. However, prior ARR-based schemes with the predefined threshold and reactive issue, which are also based on the  $REF_{prev}$ , are extremely inefficient with the RFM interface. It is because an RFM command cannot be issued in a bursty way as ARR can.

Prior ARR-based RH-protection schemes issued the ARR command whenever  $Est_{cnt}$  reaches a certain predefined threshold specified by the target  $RH_{TH}$  and type of the scheme. If we pursue the same approach to the RFM interface, we could buffer the rows’ addresses that reach a predefined threshold. Then we wait for the following RFM command to execute the  $REF_{prev}$  for the buffered victim row. If we assume an ARR-based scheme with the  $r_{blast}$  of one, the safe  $RH_{TH}$  level is 3K when the predefined threshold is 1.5K. However, the same scheme with the RFM interface of  $RFM_{TH}$  64 may have a severely degraded safe  $RH_{TH}$  level of 19K. When 300 different rows reach the activation count of 1.5K simultaneously in a tREFW time window, the last row has to wait for over 19K ( $300 \times 64$ ) ACTs until it gets its turn.

In this work, we propose to use a greedy selection of a target row at every RFM command for the RFM-based scheme. To avoid a concentration of victim rows that needs a  $REF_{prev}$ , we should preemptively refresh the rows with the highest  $Est_{cnt}$ . Based on this action, the streaming algorithm for the counter management has two requirements; 1) *Det bound-low* and 2) *Det bound-high*. *Det bound-low* is again necessary for the deterministic RH-protection guarantee. *Det bound-high* is newly required for the proper readjustment of  $Est_{cnt}$ . A similar method of  $Est_{cnt}$  adjustment as TWiCe can be applied if the lower bound of the decremented  $Real_{cnt}$  is known. Out of two possible candidates, we choose the CbS algorithm for Mithril due to its smaller area overhead compared to the Lossy-Counting algorithm (Figure 4 in Section IV-C).

#### D. Compatibility of the Grouped Counter Approach

So far, we have overlooked another method of efficient counter management, the grouped counter approach. However, the prior works that had augmented the methodology are not compatible with or efficient at the RFM interface. CBT [43] is the representative scheme of this kind. First, it cannot utilize the RFM opportunities during its tree construction phase. Suppose it chooses to prematurely refresh a group that is not fully split. In that case, it will have to refresh too many rows too conservatively. Second, even after the tree is constructed, having a leaf node of a size larger than eight rows will not fit into a single tRFM period, leading to the stacking of refresh loads. CAT-TWO [25], which extends CBT, may guarantee the leaf to be small (covering a single row) enough, but only at the cost of a higher area overhead.

#### IV. MITHRIL

Mithril is the first RFM-interface-compatible RH-protection scheme providing the deterministic protection guarantee. It exploits a modified CbS algorithm for counter management. Each entry in the counter table holds a DRAM row address and a counter value related to the address. Mithril also tracks the maximum and minimum counter entries using two pointers,  $MaxPtr$  and  $MinPtr$ , favoring the greedy selection and adjustment of the  $Est_{cnt}$ . We first only consider the  $r_{blast}$  of one. In Section V-C, we will reconsider the different  $r_{blast}$ .

##### A. Operation

Figure 3 illustrates how Mithril manages its counter structure (henceforth Mithril table) and the two pointers,  $MaxPtr$  and  $MinPtr$ . For every ACT, Mithril checks if the table already tracks the activated row address. If so, the associated counter is incremented by one. When the row address misses, the address of the entry pointed by  $MinPtr$  is replaced with the requesting row address, and its counter is incremented by one.  $MaxPtr$  and  $MinPtr$  are updated at each step to point to the correct maximum and minimum. Thus far, the operation is identical to the original CbS algorithm.

Once in every  $RFM_{TH}$  ACT, the MC issues an RFM command. At this point, Mithril selects the entry pointed by  $MaxPtr$  (greedy selection). It preemptively performs the  $REF_{prev}$  for the two victim rows associated with this entry, identified as a prime candidate of aggressor rows. Then, the counter value is decremented to the table's minimum value pointed by  $MinPtr$ .  $MaxPtr$  and  $MinPtr$  are updated correspondingly.

##### B. Brief Overview of the Proof

**Theorem.** *Mithril guarantees that the maximum increase of ACT  $Real_{cnt}$  for any single row is smaller than  $RH_{TH}/2$  during any given tREFW.*

Proving the above theorem guarantees the deterministic RH-protection at  $r_{blast}$  of one. To prove the theorem, we need to prove that 1) the modified CbS algorithm with the reset still holds and that 2) the continuous greedy selection and

preemptive refresh create an upper bound in the rate of  $Est_{cnt}$  increment. The first point is easily proved from the algorithm property. The second point, on the other hand, requires rigorous proof based on mathematical induction. In the case of the prior ARR-based schemes, proving the RH-protection from the utilized algorithm (second point) was trivial; they refresh a row whenever it reaches a predefined threshold, directly related to the target  $RH_{TH}$ . The throttling-based scheme, BlockHammer, relies on rigorous case categorization and the analytical solver in proving the RH-protection.

**Proposition 1.** *Reported  $Est_{cnt}$  is always greater than or equal to the  $Real_{cnt}$  (Det upper-bound).*

The  $Est_{cnt}$  of any address in the CbS algorithm always satisfies the inequality (1) or (2) (Section II-F). Considering Mithril operates the same as the original CbS algorithm at the ACT command, we only need to show whether the conditions hold at the RFM command. *On-table rows:* for the decremented address at RFM, inequality (1) still holds because the  $Real_{cnt}$  after the RFM command is now zero and the  $Est_{cnt}$  is  $Min$ . As for the other addresses in the table, no variable is affected. *Off-Table rows:* the addresses that are not on the table are also unaffected since such decrement does not alter the  $Min$  of inequality (2). In other words, if we had decremented  $Est_{cnt}$  lower than the  $Min$ , it would have affected the boundary of other addresses, breaking the algorithm property.

**Proposition 2.** *Within any tREFW, the increase of  $Est_{cnt}$  for any single row is bounded to  $M$ , which is a function of  $N_{entry}$  and  $RFM_{TH}$ .*

$$M = \sum_{k=1}^{N_{entry}} \frac{RFM_{TH}}{k} + \frac{RFM_{TH}}{N_{entry}} \left( \frac{tREFW(1 - \frac{tRFC}{tREF})}{tRC \times RFM_{TH} + tRFM} - 2 \right)$$

The detailed proof of Proposition 2 is provided in Appendix (Section IX). Intuitively, Mithril can limit the maximum amount of increase in accumulated ACT count on a single row through greedy selection. If a row is activated too often for a short period, it will soon become the target of the greedy selection and its victims will get refreshed. If a row is activated too rarely, the increment rate of the activation count will be low, although it can avoid being the target of  $REF_{prev}$ . The formula of  $M$  can also be interpreted as the worst-case ACT pattern with the initial condition.

Combining Proposition 1 and 2, the bound  $M$  of  $Est_{cnt}$  is also always greater than or equal to the increase in  $Real_{cnt}$ . Thus, with a properly configured  $N_{entry}$  and  $RFM_{TH}$  value that satisfies the  $M < RH_{TH}/2$ , we can prove the deterministic RH-protection.

##### C. Configuring $N_{entry}$ and $RFM_{TH}$

There are multiple possible Mithril configurations for a single target  $RH_{TH}$ , because both  $N_{entry}$  and  $RFM_{TH}$  can change to satisfy  $M < RH_{TH}/2$ . Figure 4 plots  $(N_{entry}, RFM_{TH})$  pairs that satisfy this condition for varying  $RH_{TH}$  (e.g., 1.5K, 3.125K, ..., 50K). It first shows a trade-off between



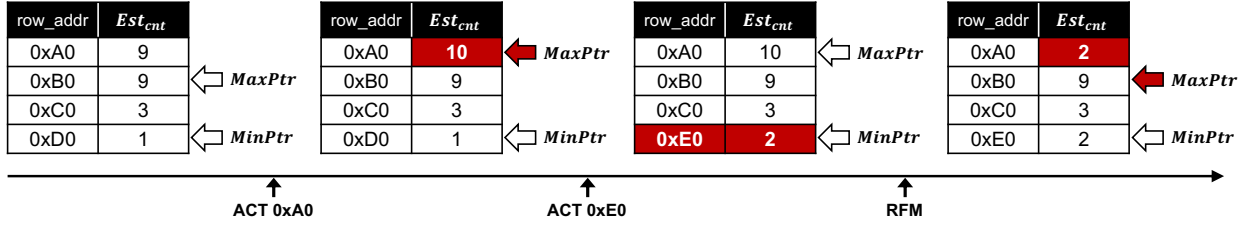


Fig. 3. A sequence of ACT and RFM commands and the corresponding update on the Mithril table.

TABLE III  
NOTATION USED IN THEOREM AND PROPOSITION

Symbol	Description
$M$	Maximum increase in an aggressor row's $Est_{cnt}$ within tREFW.
$N_{entry}$	The number of entries in the Mithril table.
$RFM_{TH}$	ACT threshold that triggers the RFM command.

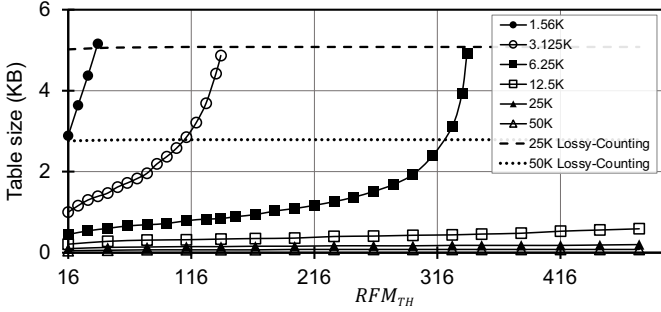


Fig. 4. Each line denotes the possible configuration of  $N_{entry}$  and  $RFM_{TH}$  that can protect against the given  $RH_{TH}$  value. RFM-based scheme built with Lossy-Counting algorithm is also denoted in dotted lines.

$N_{entry}$  and  $RFM_{TH}$  regardless of  $RH_{TH}$ . Decreased  $N_{entry}$  implies less area usage but results in the lower  $RFM_{TH}$ , implying more performance and energy overhead due to more frequent issues of RFM commands. The trade-off exists for all  $RH_{TH}$ , but the curve looks different across the various  $RH_{TH}$  values. A scheme similar to Mithril but based on the Lossy-counting algorithm is also notated at 50K and 25K  $RH_{TH}$  values, which clearly demonstrates a greater table size.

When  $RH_{TH}$  is sufficiently high (e.g., larger than 12.5K), it is possible to set  $RFM_{TH}$  to be around 256 at a relatively small  $N_{entry}$ . Then, Mithril can achieve RH-protection with a relatively low area, performance, and energy overhead. In contrast, when  $RH_{TH}$  is low, maintaining the low performance/energy overhead (i.e., sufficiently large  $RFM_{TH}$ ) requires a substantially larger  $N_{entry}$ . Overall, this is a trade-off that a DRAM vendor needs to consider when determining  $N_{entry}$ . The target  $RH_{TH}$  level can be adjusted by tweaking the  $RFM_{TH}$  value even if  $N_{entry}$  is fixed. This flexibility can be handy when the scheme has to be built based on the predicted  $RH_{TH}$  level and thus fixed area, as it can avoid excessive performance/energy overhead.

#### D. Hardware Implementation

**Mithril Hardware Overview:** The Mithril table comprises two CAM structures, each storing the row address and the activation count. A  $MaxPtr$  and  $MinPtr$  are also employed as the index pointing registers. The Mithril logic and CAM

structures must be equipped for every bank at every DRAM chip. At every ACT command, the address CAM is checked by the activated row address. Then, the count CAM,  $MaxPtr$ , and  $MinPtr$  are updated if needed. At every RFM command, the count CAM is queried by the  $MaxPtr$  pointed index and performs decrement. Then, during the tRFM time window, a new maximum value is found and updated for the  $MaxPtr$ .

**Wrapping Counter:** The absolute counter value of the Mithril table can increase unbounded during its run-time, which complicates the hardware implementation. Prior works solved this issue by periodically resetting the whole table [31], [39] or using a duplicate counter table in an interleaving fashion [50]; both are bearing a two-fold degradation of predefined threshold level (from  $RH_{TH}/2$  to  $RH_{TH}/4$ ) and area, respectively. However, Mithril can avoid this. Unlike the prior works, Mithril does not require the absolute value of  $Est_{cnt}$ . Instead, we require the *relative difference* of  $Est_{cnt}$  against the minimum  $Est_{cnt}$  on the Mithril table. Moreover, due to the operational behavior of Mithril, the maximum difference between the  $MaxPtr$  and  $MinPtr$  counter values is always bounded. Therefore, we adopt a wrapping counter for the Mithril table implementation. If we provision enough bits that can express a higher value than the maximum difference in the table, the wrapping counter can always correctly identify the relative size relationship among the Mithril table entries. Through this implementation, we acquire a two-fold benefit.

### V. MITHRIL OPTIMIZATIONS

#### A. Adaptive Refresh

In Section IV, it was assumed that Mithril performs a  $REF_{prev}$  for every RFM command. However, the other option is to selectively perform a  $REF_{prev}$  depending on the current state. Specifically, we propose to perform an additional refresh only when the difference between the  $MaxPtr$  and the  $MinPtr$  count values exceeds a certain threshold ( $Ad_{TH}$ ). We call this an *adaptive refresh policy*.

Intuitively, this effectively avoids performing the additional refresh when the memory access exhibits a pattern where no specific row is accessed much more frequently than the others in a short time window. If  $Ad_{TH}$  is chosen large enough, Mithril with the adaptive refresh policy can effectively filter out the ACT patterns observed by the normal workloads. By doing so, we can minimize the unnecessary energy overhead caused by false-alarmed refreshes. Figure 5 shows the effectiveness of the adaptive refresh policy, almost eliminating additional energy overhead with benign workloads (see Section VI for the details of the experimental setup).

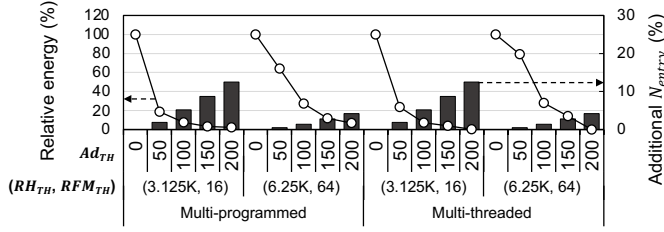


Fig. 5. Relative dynamic energy overhead against baseline with no RH-protection and relative number of  $N_{entry}$  regarding 4 different  $Ad_{TH}$  levels.

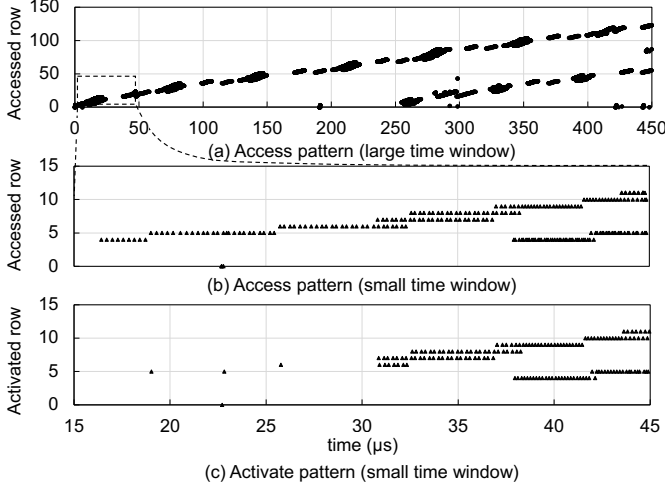


Fig. 6. Exemplar large object sweep pattern of lbm in SPEC CPU2017. (a) shows the memory access pattern in large time window. (b) is magnified to the small window. (c) shows the activation pattern in the small window.

Among the multiple  $Ad_{TH}$  values, we can identify that the adaptive refresh policy is effective at the range of 100 to 200 in all cases. We seek the root cause in the cross-play of memory access patterns of the ordinary workloads and the DRAM row size. Multithreaded or memory-intensive workloads often exhibit large-object-sweep behavior that results in main-memory accesses (Figure 6(a)). In such a case, memory access concentrates on a small number of rows in a short time period (Figure 6(b)) while being rather evenly distributed to the entire footprint in total. Although such an access pattern may possess high DRAM row locality, inter-process/thread conflict may cause a high rate of ACT per memory access (Figure 6(c)). Here, the number of concentrated ACTs would be similar to the number of streaming RDs/WRs, which would be 128 for 8KB DRAM row and 64B cache line size. This matches the value range of the effective adaptive threshold range, although the exact value must be decided empirically.

The adaptive refresh policy causes a slight deterioration on the bound  $M$ , thus inducing a higher area or performance overhead to reach the same effect as the baseline. However, such an effect is minimal unless  $Ad_{TH}$  is very high. Figure 5 shows a small increase in  $N_{entry}$ , maximum 12% only at very low  $RH_{TH}$ . The mathematical proof of the adjusted table size can be derived from Proposition 2 and conducted in Section IX-B.

TABLE IV  
ARCHITECTURAL PARAMETERS FOR SIMULATION

Core Configurations (16 cores)	
Core	3.6 GHz 4-way OOO cores
LLC	16 MB
Memory System Configurations	
Module	DDR5-4800
Channel	2 channels
Configuration	1 rank; 32 banks per rank
Scheduling	BLISS [47]
Page-Policy	Minimalist-open [26]
$t_{RFC}$ , $t_{RC}$ , $t_{RFM}$	295 ns, 48.64 ns, 97.28 ns
$t_{RCD}$ , $t_{RP}$ , $t_{CL}$	16.64 ns

### B. Mithril+

The adaptive refresh policy allows Mithril to skip  $REF_{prev}$  even when the RFM command is issued by the memory controller. By doing so, Mithril can save energy but not the performance overhead. Whether a DRAM actually performs refreshes or not, the MC will continue to issue RFM commands at every  $RFM_{TH}$  ACTs.

Inspired by such limitation, we propose an optional, more invasive extension of Mithril, named Mithril+, which prevents the MC from issuing the unnecessary RFM command. Mithril+ utilizes the mode register in the DRAM device, which is flagged when the difference between  $MaxPtr$  and  $MinPtr$  is smaller than  $Ad_{TH}$ . At every  $RFM_{TH}$ , MC reads the flag using the JEDEC-standard MRR (Mode Register Read) command, deciding whether or not to issue the RFM command. With this interface, Mithril+ can substantially minimize the performance overhead at the common case of ordinary workloads at the expense of modification to the RFM interface.

### C. Non-adjacent Row Hammer

Mithril can follow similar approaches of prior works [39], [50] in handling the non-adjacent RH, by adjusting the  $M$  value and number of rows to execute  $REF_{prev}$ . When  $r_{blast}$  is one (double-sided attack),  $M$  smaller than  $RH_{TH}/2$  is safe. However, when  $r_{blast}$  is larger,  $M$  has to be smaller than  $RH_{TH}/(\text{aggregated RH effect})$  regarding the non-adjacent aggressors. In the case of a  $r_{blast}$  of 3, the aggregated RH effect is 3.5 [50], with six victim rows to execute  $REF_{prev}$ .

## VI. EVALUATION

We evaluate the performance, energy, and area overhead of Mithril and Mithril+, in comparison with the probabilistic RFM-based scheme (henceforth PARFM), as well as prior works based on either ARR or throttling.

### A. Experimental Setup

**Methodology:** Performance overhead is evaluated based on McSimA+ [3]. Table IV summarizes the experimental setup. We use normalized IPC throughput as the performance metric. We count the number of ACT, PRE, and executed  $REF_{prev}$  to calculate the dynamic energy consumption. We first synthesize Mithril hardware module RTL implementation using TSMC 40 nm standard cell library with the Synopsys design compiler. The area overhead is scaled down to DRAM 20 nm, then again



scaled up  $10\times$  [13] to conservatively take the inferior DRAM process into account. Mithril hardware energy consumption is also derived from the synthesis.

**Workloads:** We use 1) ordinary, 2) double-sided RH, 3) multi-sided RH, 4) CBT energy adversarial, and 5) BlockHammer performance adversarial workloads for evaluation. We use both multi-programmed and multi-threaded workloads for ordinary workloads. From SPEC CPU2017, we extract 100M instruction traces [45] and render two different workloads of mix-high and mix-blend, each with 16 traces of memory-intensive and randomly selected workloads, respectively. We execute 400M instructions in total. We also evaluate 3 different multi-threaded benchmarks (FFT and RADIX from SPLASH-2 [40], PageRank from GAP [7]).

We configure the multi-sided RH attack that targets multiple victims [14], [15]. We model the CBT energy adversarial pattern as the randomized ACT pattern over the whole DRAM address space; it effectively uniformly constructs the CBT tree, making the leaf group large. The BlockHammer performance adversarial pattern is configured to blacklist specific profiled rows that share the CBF entry with the benign threads. Each is activated just enough to reach the blacklist threshold. This may effectively cause the throttling of benign workloads, especially for memory-intensive ones. Each RH attack or adversarial pattern runs simultaneously with 15 other benign workloads.

**Configurations:** We select up-to three different Mithril and Mithril+ ( $N_{entry}$ ,  $RFM_{TH}$ ) configurations for each  $RH_{TH}$ , ranging from 50K to 1.5K. At high  $RH_{TH}$  values of 50K and 25K, the  $RFM_{TH}$  is fixed to 256 given that  $N_{entry}$  is already low. At the lowest  $RH_{TH}$  of 1.5K, the  $RFM_{TH}$  is fixed to 32 because a higher  $RFM_{TH}$  value results in an overly high  $N_{entry}$ . We use 200 for  $Ad_{TH}$  as default. PARFM, similar to PARA, samples a single row that is activated in a  $RFM_{TH}$  interval and executes  $REF_{prev}$ . A new mathematical equation for the probability of failure is conducted in Section IX-C. For each target  $RH_{TH}$ , the  $RFM_{TH}$  value is fixed for PARFM to satisfy the failure probability of  $10^{-15}$  for 64 banks within a 32ms time period (tREFW). The probability degrades if the number of banks to support increases.

We also evaluate the prior ARR and throttling-based schemes. We configure TWiCe and Graphene using the equations provided in each work. We configure PARA to satisfy the same failure probability of  $10^{-15}$ . CBT is configured to follow the configurations in the original work [43].

We reconfigure the BlockHammer<sup>2</sup> to match our simulation environment and our target  $RH_{TH}$  values. For (CBF Size,  $N_{BL}$ ) pairs, we used (1K, 17.1K), (1K, 8.6K), (1K, 4.3K), (2K, 2.1K), (4K, 1.1K), and (8K, 0.49K) for the  $RH_{TH}$  from 50K to 1.5K. Under our system of 4 banks for a single thread, the number of ACTs per row easily reaches over

<sup>2</sup>BlockHammer uses a pair of interleaved counting bloom filters (CBFs) similar to the Count-min Sketch algorithm. Each CBF is reset at every CBF lifetime ( $t_{CBF}$ ), which typically matches tREFW. There exists a certain blacklist threshold ( $N_{BL}$ ) of ACT, which triggers the delay on a certain row when surpassed. Delay time ( $t_{Delay}$ ) is calculated as  $(t_{CBF} - N_{BL} \times t_{RC}) / (RH_{TH} - N_{BL})$ . Thread-level scheduling support is built on top of these to throttle the aggressor thread itself.

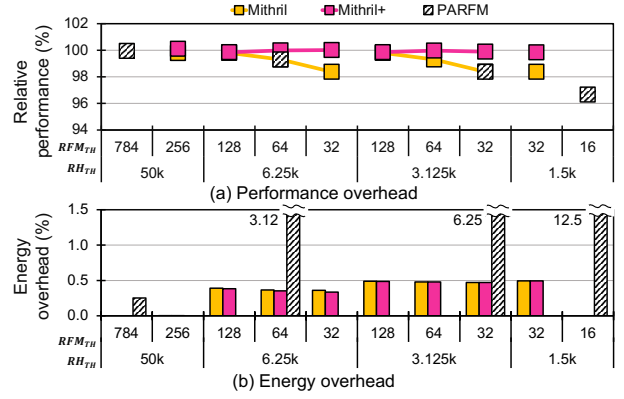


Fig. 7. The relative performance and energy overhead of Mithril, Mithril+, and PARFM. (a) 100% denotes the baseline IPC throughput without the RFM interface. (b) the additional dynamic energy overhead of the  $REF_{prev}$  and the module.

700 (as opposed to 109 ACTs in original system with more banks per thread [50]), especially for the memory-intensive workloads. Because  $N_{BL}$  must be lower than  $RH_{TH}/2$  (750 for  $RH_{TH}$  1.5K), it is difficult to set an appropriate  $N_{BL}$  value that distinguishes the benign accesses against aggressor accesses and fulfill the RH-protection at  $RH_{TH}$  1.5K, while also incurring minimal performance overhead.

#### B. RFM-based Schemes

Figure 7(a) shows the performance and energy overhead of the RFM-based schemes. Mithril+ shows near-zero performance overhead in all  $RH_{TH}$  levels. Mithril shows various performance degradation, depending on the  $RH_{TH}$  level and the configuration types. At every  $RH_{TH}$  level, Mithril with multiple configurations shows better or at least competitive performance overhead when compared with PARFM.

Figure 7(b) shows dynamic energy overhead, induced by the executed  $REF_{prev}$ . Both Mithril and Mithril+ show low overhead at all  $RH_{TH}$  levels because the properly configured  $Ad_{TH}$  value allows them to skip the majority of RFM commands in common cases. PARFM incurs much higher energy overhead as it executes  $REF_{prev}$  at every RFM command.

#### C. Comparison with the Prior Works

Figure 8 shows the performance and the energy overhead of various schemes on multiple workloads at  $RH_{TH}$  ranging from 50K to 1.5K. First, on the ordinary workloads, all the evaluated schemes show negligible performance overhead except at an extremely pessimistic  $RH_{TH}$  level of 1.5K (Figure 8(a)) for Mithril and PARA. Second, as for the double-sided and multi-sided RH attack, a similar tendency is observed in the aggregate IPC of the benign workloads, whereas the BlockHammer exhibits better throughput in most cases (Figure 8(b,c)). It is because the attacking thread is throttled by BlockHammer, favoring the benign threads. Notice that the RH attack is adversarial to Mithril, Mithril+, TWiCe, and Graphene, where Mithril executes more  $REF_{prev}$  (energy), Mithril+ issues the RFM commands more frequently (performance), and TWiCe and Graphene issue the ARR command more frequently (performance).

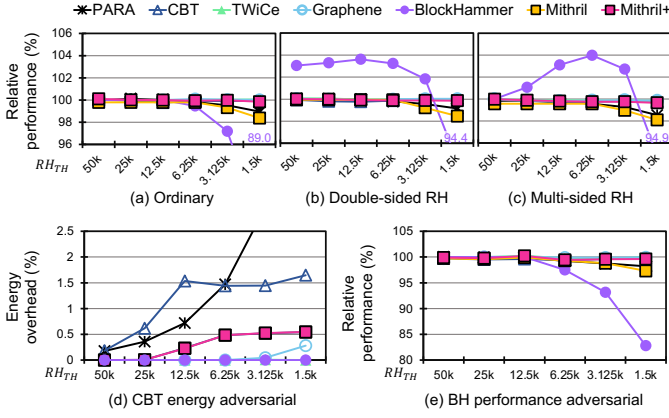


Fig. 8. (a) Relative performance at ordinary workloads. (b),(c) Relative performance of benign threads at the double-side and multi-sided RH-attack. (d) Relative dynamic energy at the CBT-adversarial pattern. (e) Relative performance of benign threads at the BlockHammer-adversarial pattern.

Third, under the CBT-energy-adversarial pattern, both CBT and PARA show high dynamic energy overhead, especially at low  $RH_{TH}$  (Figure 8(d)). PARA shows high energy overhead, regardless of the ACT pattern. CBT shows high energy overhead in this case because the largely built leaves covering several DRAM rows frequently reach the predefined threshold, resulting in a high number of  $REF_{prev}$ . Fourth, under the BlockHammer-performance-adversarial pattern, BlockHammer shows lower IPC throughput than usual (Figure 8(e)). It is because multiple rows accessed by the benign memory-intensive thread are blacklisted and thus throttled.

We report the counter table size of each scheme in *KB-per-bank* (Table V). While the MC-side scheme benefits from exploiting faster transistors, abundant wiring resources, and a relaxed area budget, the number of total banks is much higher (2048), and the target  $RH_{TH}$  value has to be pessimistic. The DRAM-side implementation can benefit from fewer banks (32) to support per device and more accurate  $RH_{TH}$  value, but is hindered by slower transistors and tighter area and wiring budget. Mithril shows lower or competitive area overhead in terms of KB per bank, reaching  $0.024mm^2$  at 6.25K  $RH_{TH}$ . It is 1% of a single DDR5 chip [27] when multiplied  $32\times$  to cover the 32 banks per chip.

All the schemes suffer from a high area or performance overhead at the  $RH_{TH}$  level of 1.5K. However, *it is possible to use the throttling-based MC-side scheme (e.g., BlockHammer) in cooperation with Mithril to avoid scalability issues*. For example, if the throttling-based scheme guarantees the  $RH_{TH}$  of 32K with low overhead, the maximum number of ACTs in a tREFW time window is reduced from 600K ( $tREFW/tRC$ ) to 32K. Because the second term of the equation for  $M$  in Proposition 2 is dominated by this,  $M$  can effectively decrease  $18\times$ , and Mithril can easily defend against a low  $RH_{TH}$  level with only a minimal area or performance overhead.

## VII. RELATED WORK

**Row Hammer on Real Systems:** As a hardware vulnerability, Row Hammer has been shown to bypass all the system

TABLE V  
PER BANK TABLE SIZE COMPARISON (KB)

Location	RH-protection Scheme	50K	25K	12.5K	6.25K	3.125K	1.5K
MC	CBT	0.47	0.97	2	4.12	8.5	17.5
	Graphene	0.14	0.21	0.51	0.99	1.92	3.7
	BlockHammer	3.75	3.5	3.25	6	11	20
Buffer Chip	TWiCe	2.79	5.08	9.54	18.27	35.29	71.26
DRAM	Mithril A	0.08	0.17	0.41	0.84	3.76	-
	Mithril B	-	-	0.3	0.68	1.78	-
	Mithril C	-	-	0.27	0.57	1.38	4.85

\* Three Mithril configurations (A,B,C) have different  $RFM_{TH}$ , from 256 to 32.

memory protection, allowing adversaries to compromise the confidentiality and integrity and confidentiality of real systems. In 2015, Google [42] demonstrated that a user-level program could breach the system-level security of a typical PC by exploiting Row Hammer vulnerability. A number of successful attacks have followed [42], including the ones compromising mobile devices [48], [49] and servers [12], [18], [41] that break the authentication process and damage the entire system, even in the case that a system protects memory locations near sensitive data [53]. Because Row Hammer undermines the fundamental principle of memory isolation, it has been regarded as a real threat drawing mitigation proposals from software, architecture, and hardware levels.

**Architectural Proposals to Mitigate Row Hammer:** There have been deterministic [25], [31], [39], [44], [50] and probabilistic [29], [46], [52] schemes proposed to mitigate Row Hammer attacks in the architecture level. Among these, [44], [46], [52] are susceptible to adversarial DRAM access patterns. TWiCe [31] and CAT-TWO [25] are relatively free from this susceptibility but require an order of magnitude more storage to track aggressor rows compared to Graphene [39]. PARA [29] incurs low performance and energy overhead, whereas it is also extremely area-efficient as it does not require counters to trace aggressor rows. Yet, the protection is probabilistic in nature; even if the probability is quite small, there is a non-zero probability that a victim row is not refreshed after reaching its Row Hammer threshold. BlockHammer [50] uses a throttling approach backed up with a thread-level MC scheduling. None of the proposals are compatible with RFM, the topic of this paper, either.

## VIII. CONCLUSION

We have proposed Mithril, a DRAM-side, RFM-compatible, energy-efficient scheme that provides deterministic safety against Row Hammer attacks. First, we show that the conventional algorithms and methodology used in the previous architectural RH-prevention schemes are not compatible with the RFM command introduced in the latest DRAM specifications, such as DDR5 and LPDDR5. By mathematical defining the maximum bound of activation count without being refreshed in a tREFW time window, we guarantee the safety on the specific  $RH_{TH}$  value. The devised adaptive refresh policy can decrease the energy overhead by exploiting the row activation patterns of ordinary workloads. Moreover, we proposed Mithril+ that requires slight modification to the memory controller operation. It utilizes the existing DRAM command to skip

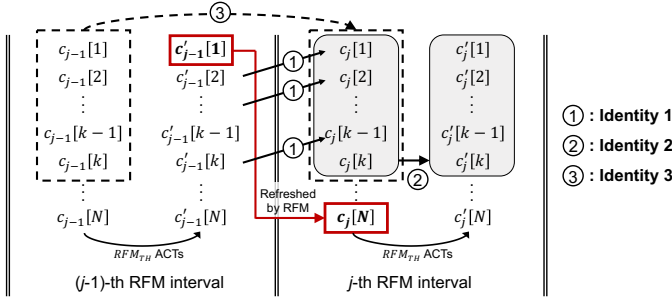


Fig. 9. Exemplar case illustrating how the  $Est_{cnt}$  is updated between two consecutive RFM intervals.

sending RFM commands, which can significantly reduce the performance overhead of the RFM interface. Our evaluation demonstrates that Mithril achieves a significantly low energy overhead in all cases compared to the PARA tailored to support RFM, whereas suffering from a higher performance overhead. Mithril+ shows not only a low energy overhead but also a significantly lower performance overhead, to be comparable to Graphene, a state-of-the-art RH-prevention scheme which is not supporting RFM.

## IX. APPENDIX

### A. Proof for Proposition 2

**Proposition 2.** *Within any tREFW, the increase of  $Est_{cnt}$  for any single row is bounded to  $M$ , which is a function of  $N_{entry}$  and  $RFM_{TH}$ .*

$$M = \sum_{k=1}^{N_{entry}} \frac{RFM_{TH}}{k} + \frac{RFM_{TH}}{N_{entry}} \left( \frac{tREFW(1 - \frac{tRFC}{tREFI})}{tRC \times RFM_{TH} + tRFM} - 2 \right)$$

Henceforth,  $N_{entry}$  is replaced by  $N$ . Also,  $W$  represents the maximum number of RFM intervals (the period between two consecutive RFM commands) between consecutive auto-refreshes and is computed as follows:

$$W = \lceil (tREFW - (tREFW/tREFI) \times tRFC) / (tRC \times RFM_{TH} + tRFM) \rceil$$

Suppose that  $c_j[i]$  is the  $i$ -th largest  $Est_{cnt}$  in the Mithril table at the beginning of  $j$ -th RFM interval ( $1 \leq i \leq N, 1 \leq j \leq W$ ).  $c'_j[i]$  is the  $i$ -th largest  $Est_{cnt}$  in the table at the end of the  $j$ -th RFM interval. Figure 9 illustrates the exemplar case for these notations. Then, the following identities hold true.

**Identity 1.**  $c'_j[i] = c_{j+1}[i - 1]$

**Proof:** At the end of each RFM interval, an entry with the largest  $Est_{cnt}$  (i.e.,  $c'_j[1]$ ) becomes the target for the RFM refresh, and its  $Est_{cnt}$  is reset to the minimum count in the table. Thus, the ranks of all the other entries promote by one after the RFM refresh.

**Identity 2.**  $\sum_{i=1}^k c'_j[i] \leq \sum_{i=1}^k c_j[i] + RFM_{TH}$  for  $1 \leq k \leq N$

**Proof:** Using the fact that there are  $RFM_{TH}$  ACTs within each RFM interval and  $c'_j[i]$  is larger than  $c_j[i]$  for all  $i$  by definition, the following holds true.

$$\begin{aligned} \sum_{i=1}^k c'_j[i] &= \sum_{i=1}^N c_j[i] - \sum_{i=k+1}^N c'_j[i] + RFM_{TH} \\ &\leq \sum_{i=1}^k c_j[i] - \sum_{i=k+1}^N c_j[i] - c'_j[i] + RFM_{TH} \leq \sum_{i=1}^k c_j[i] + RFM_{TH} \end{aligned}$$

**Identity 3.**  $\sum_{i=1}^k c_j[i] \leq \sum_{i=1}^k c_{j-1}[i] + RFM_{TH}$  for  $1 \leq k \leq N$

**Proof:** This is an obvious extension from Identity 2 because  $\sum_{i=1}^k c_j[i] \leq \sum_{i=1}^k c'_{j-1}[i]$ . In other words, an RFM refresh always decreases the sum of top  $k$  counter values in the table.

**Identity 4.**  $\sum_{i=1}^{k-1} c_j[i] \leq \frac{k-1}{k} (\sum_{i=1}^k c_{j-1}[i] + RFM_{TH})$  for  $2 \leq k \leq N$

**Proof:** Using Identity 1, Identity 2, and the fact that  $c'_{j-1}[1] \geq c'_{j-1}[i]$  for all  $i$ , the following holds true:

$$\sum_{i=1}^{k-1} c_j[i] = \sum_{i=2}^k c'_{j-1}[i] \leq \frac{k-1}{k} \sum_{i=1}^k c'_{j-1}[i] \leq \frac{k-1}{k} \left( \sum_{i=1}^k c_{j-1}[i] + RFM_{TH} \right)$$

With these identities, we are ready to prove Proposition 2. Proving Proposition 2 is equivalent to proving the following:

$$c'_W[1] - c_1[N] \leq M \text{ for given } c_1[1], \dots, c_1[N]$$

This is because any row's  $Est_{cnt}$  that is increased during the  $W$  RFM intervals is obviously less than difference between the largest  $Est_{cnt}$  at the end ( $c'_W[1]$ ) and the smallest  $Est_{cnt}$  at the beginning ( $c_1[N]$ ). Then, we can obtain the upper bound for  $c'_W[1]$  through the following:

$$\begin{aligned} c'_W[1] &\leq c_W[1] + RFM_{TH} \quad (\because \text{Identity 2}) \\ &\leq \frac{1}{2} \left( \sum_{i=1}^2 c_{W-1}[i] + RFM_{TH} \right) + RFM_{TH} \quad (\because \text{Identity 4}) \\ &\leq \frac{1}{3} \left( \sum_{i=1}^3 c_{W-2}[i] + RFM_{TH} \right) + \sum_{k=1}^2 \frac{RFM_{TH}}{k} \quad (\because \text{Identity 4}) \end{aligned}$$

Repeatedly applying Identity 4 for a total of  $N$  times, we get the following inequality:

$$\begin{aligned} c'_W[1] &\leq \frac{1}{N} \left( \sum_{i=1}^N c_{W-N+1}[i] + RFM_{TH} \right) + \sum_{k=1}^{N-1} \frac{RFM_{TH}}{k} \\ &= \frac{1}{N} \left( \sum_{i=1}^N c_{W-N+1}[i] \right) + \sum_{k=1}^N \frac{RFM_{TH}}{k} \end{aligned}$$

At this point, we cannot apply Identity 4 anymore, but instead apply Identity 3 ( $k = N$ ) for  $W - N$  times.

$$\begin{aligned} c'_W[1] &\leq \frac{\sum_{i=1}^N c_1[i]}{N} + \frac{(W - N)RFM_{TH}}{N} + \sum_{k=1}^N \frac{RFM_{TH}}{k} \\ &= \frac{\sum_{i=1}^N c_1[i]}{N} + M - \frac{N-2}{N} (RFM_{TH} - 1) \end{aligned}$$

Earlier, we showed that proving Proposition 2 is equivalent to proving  $c'_W[1] - c_1[N] \leq M$ . With the above equation, proving the following is the only step left to prove Proposition 2:

$$\frac{\sum_{i=1}^N c_1[i]}{N} - c_1[N] \leq \frac{N-2}{N} RFM_{TH}$$

Here, the left hand side can be represented as follows.

$$\frac{\sum_{i=1}^N c_1[i]}{N} - c_1[N] = \frac{\sum_{i=1}^N c_1[i] - Nc_1[N]}{N} = \frac{\sum_{i=1}^N (c_1[i] - c_1[N])}{N}$$

The upper bound of  $\sum_{i=1}^N (c_j[i] - c_j[N])$  for any  $j$ -th RFM interval can be obtained by contradiction. Assume that  $\sum_{i=1}^N (c_j[i] - c_j[N])$  is maximum when  $j$  is  $m$ , and the difference between  $c_m[1]$  and  $c_m[N]$  is greater than  $RFM_{TH}$ . Then

$$\begin{aligned} c'_{m-1}[1] - c'_{m-1}[N] &\geq c'_{m-1}[2] - c'_{m-1}[N] \\ &= c_m[1] - c_m[N] > RFM_{TH} \quad (3) \end{aligned}$$

At the end of the  $(m-1)$ -th RFM interval,  $c'_{m-1}[1]$  is reduced to  $c'_{m-1}[N]$  by RFM. Therefore

$$\begin{aligned} \sum_{i=1}^N (c_m[i] - c_m[N]) &= \sum_{i=1}^N (c'_{m-1}[i] - c'_{m-1}[N]) - (c'_{m-1}[1] - c'_{m-1}[N]) \\ &= \sum_{i=1}^N (c_{m-1}[i] - c_{m-1}[N]) + RFM_{TH} - (c'_{m-1}[1] - c'_{m-1}[N]) \\ &< \sum_{i=1}^N (c_{m-1}[i] - c_{m-1}[N]) \quad (\because (3)) \end{aligned}$$

This contradicts that  $\sum_{i=1}^N (c_j[i] - c_j[N])$  is maximum when  $j$  is  $m$ . Therefore, if  $\sum_{i=1}^N (c_j[i] - c_j[N])$  is maximum when  $j$  is  $m$ , the difference between  $c_m[1]$  and  $c_m[N]$  is less than or equal to  $RFM_{TH}$ . Then, we get the following inequality:

$$\begin{aligned} \frac{\sum_{i=1}^N (c_1[i] - c_1[N])}{N} &\leq \frac{\sum_{i=1}^N (c_m[i] - c_m[N])}{N} \\ &= \frac{\sum_{i=1}^{N-2} (c_m[i] - c_m[N])}{N} \quad (\because c_m[N-1] = c_m[N]) \\ &\leq \frac{\sum_{i=1}^{N-2} (c_m[1] - c_m[N])}{N} \\ &\leq \frac{(N-2)RFM_{TH}}{N} \end{aligned}$$

### B. Finding New $M$ for Adaptive Refresh

If the adaptive refresh policy (Section V-A) is applied to Mithril, Identity 1 and 4 in Section IX-A no longer hold because  $REF_{prev}$  may not occur at the end of the RFM interval. The modified  $M$  (henceforth  $M'$ ) for adaptive refresh is as follows.

**Proposition 3.** When the adaptive refresh is applied to Mithril, the increase of  $Est_{cnt}$  for any single row within any  $tREFW$  is bounded to  $M'$ , which is a function of  $N_{entry}$ ,  $RFM_{TH}$ , and  $Ad_{TH}$ .

$$\begin{aligned} M' &= \sum_{k=1}^n \frac{RFM_{TH}}{k} + \frac{(W - n^* + N_{entry} - 2)RFM_{TH} + (N_{entry} - n^*)Ad_{TH}}{N_{entry}} \\ * W &= \lceil (tREFW - (tREFW/tREFI) \times tRFC) / (tRC \times RFM_{TH} + tRFM) \rceil \\ * n^* &= \lceil (N_{entry} \times RFM_{TH}) / (RFM_{TH} + Ad_{TH}) \rceil \end{aligned}$$

At the end of any  $j$ -th RFM interval,  $REF_{prev}$  does not occur if the difference between  $c'_j[1]$  and  $c'_j[N]$  is less than  $Ad_{TH}$ . Considering that  $REF_{prev}$  may not occur, we modify Identity 4 to Identity 5 and 6 as follows:

**Identity 5.** If  $c'_{j-1}[1] - c'_{j-1}[N] > Ad_{TH}$ , then  $\sum_{i=1}^k c_j[i] \leq \frac{k}{k+1} (\sum_{i=1}^{k+1} c_{j-1}[i] + RFM_{TH})$  for  $1 \leq k \leq N-1$

**Proof:** If  $c'_{j-1}[1] - c'_{j-1}[N] > Ad_{TH}$ ,  $REF_{prev}$  occurs at the end of the  $(j-1)$ -th RFM interval, so we can derive the same result as Identity 4.

**Identity 6.** If  $c'_{j-1}[1] - c'_{j-1}[N] \leq Ad_{TH}$ , then  $\sum_{i=1}^k c_j[i] \leq \frac{k}{N} (\sum_{i=1}^N c_{j-1}[i] + RFM_{TH} + (N-k)Ad_{TH})$  for  $1 \leq k \leq N-1$

**Proof:** Because RFM does not occur at the  $j$ -th RFM interval,  $c_j[i] = c'_{j-1}[i]$  for  $1 \leq i \leq N$ . Then, the following holds true.

$$\begin{aligned} \sum_{i=1}^N c_j[i] &= \sum_{i=1}^N c'_{j-1}[i] \\ &= \sum_{i=1}^k c'_{j-1}[i] + \sum_{i=k+1}^N c'_{j-1}[i] \\ &\geq \sum_{i=1}^k c'_{j-1}[i] + (N-k)c'_{j-1}[N] \\ &\geq \sum_{i=1}^k c'_{j-1}[i] + (N-k)(c'_{j-1}[1] - Ad_{TH}) \\ &\geq \sum_{i=1}^k c'_{j-1}[i] + (N-k) \left( \frac{1}{k} \sum_{i=1}^k c'_{j-1}[i] - Ad_{TH} \right) \\ &\geq \frac{N}{k} \sum_{i=1}^k c'_{j-1}[i] - (N-k)Ad_{TH} \\ \sum_{i=1}^k c_j[i] &= \sum_{i=1}^k c'_j[i] \\ &\leq \frac{k}{N} \left( \sum_{i=1}^N c'_{j-1}[i] + (N-k)Ad_{TH} \right) \\ &\leq \frac{k}{N} \left( \sum_{i=1}^N c_{j-1}[i] + RFM_{TH} + (N-k)Ad_{TH} \right) \end{aligned}$$

Similar to Proposition 2, proving Proposition 3 is equivalent to proving  $c'_W[1] - c_1[N] \leq M'$ . For some arbitrary number  $n$  smaller than  $W$ , assume that  $REF_{prev}$  does not occur at the  $n$ -th last RFM interval (i.e., the  $(W-n)$ -th RFM interval) and that  $REF_{prev}$  occurs at all the subsequent RFM intervals. Even with the adaptive refresh, Identity 2 and 3 are still true.

If  $n$  is greater than  $N$ , the upper bound of  $c'_W[1] - c_1[N]$  is equivalent to  $M$  (the result of Proposition 2). We can obtain this result by applying Identity 5 (equivalent to Identity 4) for  $N$  times and applying Identity 3 for  $(W-N)$  times to  $c'_W[1]$ .

Otherwise, if  $n$  is less than or equal to  $N$ , we first repeatedly apply Identity 5 for a total of  $(n-1)$  times to obtain the upper bound of  $c'_W[1]$ :

$$\begin{aligned} c'_W[1] &\leq c_W[1] + RFM_{TH} \quad (\because \text{Identity 2}) \\ &\leq \frac{1}{2} \left( \sum_{i=1}^2 c_{W-1}[i] + RFM_{TH} \right) + RFM_{TH} \quad (\because \text{Identity 5}) \\ &\leq \frac{1}{3} \left( \sum_{i=1}^3 c_{W-2}[i] + RFM_{TH} \right) + \sum_{k=1}^2 \frac{RFM_{TH}}{k} \quad (\because \text{Identity 5}) \\ &\vdots \\ &\leq \frac{1}{n} \left( \sum_{i=1}^n c_{W-n+1}[i] + RFM_{TH} \right) + \sum_{k=1}^{n-1} \frac{RFM_{TH}}{k} \\ &= \frac{1}{n} \left( \sum_{i=1}^n c_{W-n+1}[i] \right) + \sum_{k=1}^n \frac{RFM_{TH}}{k} \end{aligned}$$

At this point, we have to apply Identity 6.

$$c'_W[1] \leq \frac{1}{N} \left( \sum_{i=1}^N c_{W-n}[i] + RFM_{TH} + (N-n)Ad_{TH} \right) + \sum_{k=1}^n \frac{RFM_{TH}}{k}$$

Then, we apply Identity 3 ( $k = N$ ) for  $(W-n)$  times.

$$c'_W[1] \leq \frac{1}{N} \left( \sum_{i=1}^N c_1[i] + (W-n)RFM_{TH} + (N-n)Ad_{TH} \right) + \sum_{k=1}^n \frac{RFM_{TH}}{k}$$

The maximum value of  $\sum_{i=1}^N (c_j[i] - c_j[N])$  is equivalent to that in the proof of Proposition 2. Then, the following holds true.

$$\begin{aligned} c'_W[1] - c'_W[N] &\leq \frac{1}{N} \left( \sum_{i=1}^N (c_1[i] - c_1[N]) + (W - n)RFM_{TH} + (N - n)Ad_{TH} \right) \\ &\quad + \sum_{k=1}^n \frac{RFM_{TH}}{k} \\ &\leq \frac{1}{N} ((N - 2)RFM_{TH} + (W - n)RFM_{TH} + (N - n)Ad_{TH}) \\ &\quad + \sum_{k=1}^n \frac{RFM_{TH}}{k} \\ &\leq \frac{1}{N} ((N - 2 + W - n)RFM_{TH} + (N - n)Ad_{TH}) + \sum_{k=1}^n \frac{RFM_{TH}}{k} \quad (4) \end{aligned}$$

Suppose that  $M'[n]$  is the right side of the inequality (4) for  $1 \leq n \leq N$ . Note that  $M'[N] = M$ , which is the upper bound of  $c'_W[1] - c_1[N]$  when  $n$  is greater than  $N$  (which is the same as the value when the adaptive refresh is not applied). Now, we need to find the  $n$  value maximizing  $M'[n]$ . For  $2 \leq n \leq N$ , the difference between  $M'[n]$  and  $M'[n - 1]$  is as follows:

$$M'[n] - M'[n - 1] = \frac{RFM_{TH}}{n} - \frac{RFM_{TH} + Ad_{TH}}{N}$$

$(M'[n] - M'[n - 1])$  is a decreasing function with respect to  $n$ . Thus, the largest  $n$  (i.e.,  $n^*$ ) satisfying  $M'[n] > M'[n - 1]$  is given by  $n^* = \lceil (N \times RFM_{TH}) / (RFM_{TH} + Ad_{TH}) \rceil$ , and it maximizes  $M'[n]$ . Finally, we can prove Proposition 3 as follows:

$$\begin{aligned} c'_W[1] - c'_W[N] &\leq \sum_{k=1}^{n^*} \frac{RFM_{TH}}{k} + \frac{(W - n^* + N - 2)RFM_{TH} + (N - n^*)Ad_{TH}}{N} \\ &= M' \\ * \quad M' &= M'[n^*] \end{aligned}$$

### C. PARFM Probability of Failure

A PARA-inspired, intuitive form of a probabilistic prevention scheme PARFM is deployable under the RFM interface. Whenever an RFM command arrives, PARFM randomly samples a single aggressor row among the last  $RFM_{TH}$  activations and executes the  $REF_{prev}$  on its victims. The probability of being selected for a row depends on the ratio of its ACTs on the last  $RFM_{TH}$  activations. PARFM's protection capability depends on  $RFM_{TH}$ , which determines the sampling rate.

Failure probability of PARFM requires two major modifications on the original method of PARA: *the worst-case ACT pattern* and *mathematical formulation*. First, the number of rows to activate depends on the given  $RFM_{TH}$  value, while the worst-case ACT pattern of PARA was to activate a single row continuously. Suppose only a single row is activated under PARFM. In that case, it will always be selected at the next RFM command, and its victims will receive  $REF_{prev}$ . From the attacker's perspective, the cost-effectiveness in minimizing the PARFM selection and quickly reaching  $RH_{TH}$  is expressed as follows (where  $j$  denotes the number of ACTs for a single row in a single  $RFM_{TH}$  activation interval):

$$\text{Cost-effectiveness: } \left( 1 - \frac{j}{RFM_{TH}} \right)^{1/j} \quad (5)$$

Because this is a monotonically decreasing function and the  $RFM_{TH}$  period that the row is not activated can be ignored (it

does not contribute to reaching the  $RH_{TH}$  ACTs), activating a row only a single time for every  $RFM_{TH}$  is the most cost-effective pattern. We thus base our further formulation on that the  $RFM_{TH}$  number of different rows are activated once every  $RFM_{TH}$  period.

Compared to PARA, the mathematical formula also must be different. The following formula is the accurate probability of failure for a single DRAM bank in a tREFW time window.  $Fail(1)$  denotes the failure probability where a single row fails.  $Fail(2)$  denotes the failure probability where two different rows fail in a tREFW window and so on. Based on Equation (5), a uniform distribution of ACTs on the activated rows is assumed.

$$\begin{aligned} \text{Bank failure probability: } &_{RFM_{TH}} C_1 Fail(1) - _{RFM_{TH}} C_2 Fail(2) \\ &+ _{RFM_{TH}} C_3 Fail(3) - _{RFM_{TH}} C_4 Fail(4) \dots \end{aligned}$$

$Fail(1)$  can be calculated using the following recurrence equation where  $P[i]$  denotes the failure probability at the  $i$ -th RFM command:

$$P[i] = P[i - 1] + \frac{1}{RFM_{TH}} \left( 1 - \frac{1}{RFM_{TH}} \right)^{RH_{TH}/2} (1 - P[i - RH_{TH}/2 - 1])$$

The initial condition is as follows.

$$P[i] = \begin{cases} 0 & \text{for } 0 \leq i \leq \frac{RH_{TH}}{2} - 1 \\ \left( 1 - \frac{1}{RFM_{TH}} \right)^{RH_{TH}/2} & \text{for } i = \frac{RH_{TH}}{2} \end{cases}$$

We acquire  $Fail(1)$  by calculating the last  $P[i]$  in a tREFW window.  $Fail(2)$  is much smaller than  $Fail(1)$  because the  $RH_{TH}$  value exceeds over 1K even at the most pessimistic RH vulnerability. The probability of more than one row reaching the  $RH_{TH}$  ACT value without being refreshed is much less likely compared to that of a single row. Therefore, we estimate the (upper-bound) probability of failure with only the first term of bank failure probability. Using the bank failure probability, we can acquire the system failure probability based on the number of banks that can be simultaneously attacked ( $N_{banks}$ ).

$$\text{System Failure Probability: } 1 - (1 - Fail(1))^{N_{banks}}$$

In our experimental system of 2 ranks of 32 banks each, total 22 banks can be activated satisfying the tFAW constraints. In Section VI-A, we properly set the  $RFM_{TH}$  value on each target  $RH_{TH}$ ; therefore, our system failure probability is lower than  $10^{-15}$ .

### REFERENCES

- [1] M. T. Aga, Z. B. Aweke, and T. Austin, "When good protections go bad: Exploiting anti-dos measures to accelerate rowhammer attacks," in *2017 IEEE International Symposium on Hardware Oriented Security and Trust (HOST)*. IEEE, 2017, pp. 8–13.
- [2] P. K. Agarwal, G. Cormode, Z. Huang, J. M. Phillips, Z. Wei, and K. Yi, "Mergeable summaries," *ACM Transactions on Database Systems (TODS)*, vol. 38, no. 4, pp. 1–28, 2013.
- [3] J. Ahn, S. Li, S. O., and N. P. Jouppi, "McSimA+: A manycore simulator with application-level+ simulation and detailed microarchitecture modeling," in *IEEE International Symposium on Performance Analysis of Systems and Software*, 2013.
- [4] Apple Inc., "About the security content of Mac EFI Security Update 2015-001," <https://support.apple.com/en-us/HT204934>, 2015.



- [5] Z. B. Aweke, S. F. Yitbarek, R. Qiao, R. Das, M. Hicks, Y. Oren, and T. Austin, "ANVIL: Software-Based Protection Against Next-Generation Rowhammer Attacks," in *Proceedings of the 21st International Conference on Architectural Support for Programming Languages and Operating Systems*, 2016.
- [6] R. Balasubramonian, *Innovations in the Memory System*. Morgan & Claypool Publishers, 2019.
- [7] S. Beamer, K. Asanovic, and D. A. Patterson, "The GAP Benchmark Suite," *ArXiv*, 2015.
- [8] I. Bhati, M. Chang, Z. Chishti, S. Lu, and B. Jacob, "DRAM Refresh Mechanisms, Penalties, and Trade-Offs," *IEEE Transactions on Computers*, 2016.
- [9] F. Brasser, L. Davi, D. Gens, C. Liebchen, and A.-R. Sadeghi, "CAN'T Touch This: Software-only Mitigation Against Rowhammer Attacks Targeting Kernel Memory," in *26th USENIX Conference on Security Symposium*, 2017.
- [10] M. Charikar, K. Chen, and M. Farach-Colton, "Finding Frequent Items in Data Streams," in *Proceedings of the 29th International Colloquium on Automata, Languages and Programming*, 2002.
- [11] L. Cojocar, J. Kim, M. Patel, L. Tsai, S. Saroiu, A. Wolman, and O. Mutlu, "Are we susceptible to rowhammer? an end-to-end methodology for cloud providers," in *IEEE Symposium on Security and Privacy (S&P)*, 2020.
- [12] L. Cojocar, K. Razavi, C. Giuffrida, and H. Bos, "Exploiting correcting codes: On the effectiveness of ecc memory against rowhammer attacks," in *IEEE Symposium on Security and Privacy (S&P)*, 2019.
- [13] F. Devaux, "The true processing in memory accelerator," in *2019 IEEE Hot Chips 31 Symposium (HCS)*. IEEE Computer Society, 2019, pp. 1–24.
- [14] P. Frigo, E. Vannacci, H. Hassan, V. van der Veen, O. Mutlu, C. Giuffrida, H. Bos, and K. Razavi, "Trespass: Exploiting the many sides of target row refresh," in *S&P*, May 2020.
- [15] "'half-double': Next-row-over assisted rowhammer," [https://github.com/google/hammer-kit/blob/main/20210525\\_half\\_double.pdf](https://github.com/google/hammer-kit/blob/main/20210525_half_double.pdf), Google, 2021.
- [16] Z. Greenfield and L. Tomer, "Throttling support for row-hammer counters," Feb. 2 2016, uS Patent 9,251,885.
- [17] D. Gruss, M. Lipp, M. Schwarz, D. Genkin, J. Juffinger, S. O'Connell, W. Schoecl, and Y. Yarom, "Another flip in the wall of rowhammer defenses," *S&P*, 2017.
- [18] D. Gruss, C. Maurice, and S. Mangard, "Rowhammer.js: A remote software-induced fault attack in javascript," in *Detection of Intrusions and Malware, and Vulnerability Assessment*, 2016.
- [19] G. Irazoqui, T. Eisenbarth, and B. Sunar, "MASCAT: Preventing Microarchitectural Attacks Before Distribution," in *Proceedings of the 8th ACM Conference on Data and Application Security and Privacy*, 2018.
- [20] JEDEC, "DDR4 SDRAM Standard," 2017.
- [21] JEDEC, "LPDDR5 standard JESD209-5," 2019.
- [22] JEDEC, "DDR5 SDRAM," 2020.
- [23] JEDEC, "NEAR-TERM DRAM LEVEL ROWHAMMER MITIGATION," 2021.
- [24] JEDEC, "SYSTEM LEVEL ROWHAMMER MITIGATION," 2021.
- [25] I. Kang, E. Lee, and J. Ahn, "CAT-TWO: Counter-Based Adaptive Tree, Time Window Optimized for DRAM Row-Hammer Prevention," *IEEE Access*, vol. 8, pp. 17 366–17 377, 2020.
- [26] D. Kaseridis, J. Stuecheli, and L. K. John, "Minimalist open-page: A DRAM page-mode scheduling policy for the many-core era," in *44th Annual IEEE/ACM International Symposium on Microarchitecture*, 2011.
- [27] D. Kim, M. Park, S. Jang, J.-Y. Song, H. Chi, G. Choi, S. Choi, J. Kim, C. Kim, K. Kim *et al.*, "23.2 a 1.1 v 1nm 6.4 gb/s/pin 16gb ddr5 sdram with a phase-rotator-based dll, high-speed serdes and rx/tx equalization scheme," in *2019 IEEE International Solid-State Circuits Conference (ISSCC)*. IEEE, 2019, pp. 380–382.
- [28] J. Kim, M. Patel, A. G. Yaglikci, H. Hassan, R. Azizi, L. Orosa, and O. Mutlu, "Revisiting rowhammer: An experimental analysis of modern dram devices and mitigation techniques," in *Proceedings of the 47th Annual International Symposium on Computer Architecture*, 2020.
- [29] Y. Kim, R. Daly, J. Kim, C. Fallin, J. H. Lee, D. Lee, C. Wilkerson, K. Lai, and O. Mutlu, "Flipping Bits in Memory Without Accessing Them: An Experimental Study of DRAM Disturbance Errors," in *Proceeding of the 41st Annual International Symposium on Computer Architecture*, 2014.
- [30] R. K. Konoth, M. Oliverio, A. Tatar, D. Andriesse, H. Bos, C. Giuffrida, and K. Razavi, "ZebRAM: Comprehensive and Compatible Software Protection Against Rowhammer Attacks," in *13th USENIX Symposium on Operating Systems Design and Implementation*, 2018.
- [31] E. Lee, I. Kang, S. Lee, G. E. Suh, and J. Ahn, "TWiCe: Preventing Row-hammering by Exploiting Time Window Counters," in *Proceedings of the 46th International Symposium on Computer Architecture*, 2019.
- [32] G. S. Manku and R. Motwani, "Approximate Frequency Counts over Data Streams," in *Proceedings of the 28th International Conference on Very Large Data Bases*, 2002.
- [33] A. Metwally, D. Agrawal, and A. El Abbadi, "Efficient Computation of Frequent and Top-k Elements in Data Streams," in *Proceedings of the 10th International Conference on Database Theory*, 2005.
- [34] J. Misra and D. Gries, "Finding repeated elements," *Science of Computer Programming*, vol. 2, no. 2, 1982.
- [35] S. Muthukrishnan, *Data streams: Algorithms and applications*. Now Publishers Inc, 2005.
- [36] O. Mutlu and J. S. Kim, "RowHammer: A Retrospective," *IEEE Transactions on Computer-Aided Design of Integrated Circuits and Systems*, 2019.
- [37] B. Nale and C. E. Cox, "Refresh command control for host assist of row hammer mitigation," Jul. 25 2019, uS Patent App. 16/370,578.
- [38] K. Park, C. Lim, D. Yun, and S. Baeg, "Experiments and root cause analysis for active-precharge hammering fault in ddr3 sdram under 3x nm technology," *Microelectronics Reliability*, 2016.
- [39] Y. Park, W. Kwon, E. Lee, T. J. Ham, J. Ahn, and J. W. Lee, "Graphene: Strong yet Lightweight Row Hammer Protection," in *MICRO*, 2020.
- [40] PARSEC Group, "A Memo on Exploration of SPLASH-2 Input Sets," in *Princeton University*, 2011.
- [41] K. Razavi, B. Gras, E. Bosman, B. Preneel, C. Giuffrida, and H. Bos, "Flip feng shui: Hammering a needle in the software stack," in *USENIX Conference on Security Symposium*, 2016.
- [42] M. Seaborn and T. Dullien, "Exploiting the DRAM Rowhammer Bug to Gain Kernel Privileges," <https://googleprojectzero.blogspot.com/2015/03/exploiting-dram-rowhammer-bug-to-gain.html>, 2015.
- [43] S. M. Seyedzadeh, A. K. Jones, and R. Melhem, "Counter-Based Tree Structure for Row Hammering Mitigation in DRAM," *IEEE Computer Architecture Letters*, 2017.
- [44] S. M. Seyedzadeh, A. K. Jones, and R. Melhem, "Mitigating Wordline Crosstalk Using Adaptive Trees of Counters," in *ISCA*, 2018.
- [45] T. Sherwood, E. Perelman, G. Hamerly, and B. Calder, "Automatically Characterizing Large Scale Program Behavior," in *Proceedings of the 10th International Conference on Architectural Support for Programming Languages and Operating Systems*, 2002.
- [46] M. Son, H. Park, J. Ahn, and S. Yoo, "Making DRAM Stronger Against Row Hammering," in *Proceedings of the 54th Annual Design Automation Conference*, 2017.
- [47] L. Subramanian, D. Lee, V. Seshadri, H. Rastogi, and O. Mutlu, "Bliss: Balancing performance, fairness and complexity in memory access scheduling," *IEEE Transactions on Parallel and Distributed Systems*, vol. 27, no. 10, pp. 3071–3087, 2016.
- [48] V. van der Veen, Y. Fratantonio, M. Lindorfer, D. Gruss, C. Maurice, G. Vigna, H. Bos, K. Razavi, and C. Giuffrida, "Drammer: Deterministic Rowhammer Attacks on Mobile Platforms," in *Proceedings of the 2016 ACM SIGSAC Conference on Computer and Communications Security*, 2016.
- [49] V. van der Veen, M. Lindorfer, Y. Fratantonio, H. Pillai, G. Vigna, C. Kruegel, H. Bos, and K. Razavi, "GuardiON: Practical mitigation of dma-based rowhammer attacks on ARM," in *15th International Conference on Detection of Intrusions and Malware, and Vulnerability Assessment (DIMVA)*, 2018.
- [50] A. G. Yaglikci, M. Patel, J. Kim, R. AziziBarzoki, J. Park, H. Hassan, A. Olgun, L. Orosa, K. Kanellopoulos, T. Shahroodi, S. Ghose, and O. Mutlu, "Blockhammer: Preventing rowhammer at low cost by blacklisting rapidly-accessed dram rows," in *International Symposium on High-Performance Computer Architecture*, 2021.
- [51] T. Yang and X. Lin, "Trap-Assisted DRAM Row Hammer Effect," *IEEE Electron Device Letters*, 2019.
- [52] J. M. You and J.-S. Yang, "MRLoc: Mitigating Row-hammering Based on Memory Locality," in *Proceedings of the 56th Annual Design Automation Conference*, 2019.
- [53] Z. Zhang, Y. Cheng, D. Liu, S. Nepal, Z. Wang, and Y. Yarom, "PThammer: Cross-User-Kernel-Boundary Rowhammer through Implicit Accesses," in *MICRO*, 2020.